# Electric-field and current-induced metastability and resistivity relaxation in $La_{0.8}Ca_{0.2}MnO_3$ at low temperatures

V. Markovich, G. Jung, Y. Yuzhelevski, and G. Gorodetsky
*Department of Physics, Ben Gurion University of the Negev, P.O. BOX 653, 84105 Beer Sheva, Israel*

A. Szewczyk and M. Gutowska
*Instytut Fizyki PAN, 02 668 Warszawa, Poland*

D. A. Shulyatev and Ya. M. Mukovskii
*Moscow State Steel and Alloys Institute, 117936, Moscow, Russia*

(Received 13 April 2004; revised manuscript received 7 June 2004; published 20 August 2004)

Transport, magnetic, and thermal properties of phase-separated $La_{0.8}Ca_{0.2}MnO_3$ crystal were studied in a wide temperature range down to 10 K. At low temperatures below the Curie point $T_C=184$ K, the sample resistance is characterized by spontaneous transitions to higher resistivity metastable states. Metastability becomes more pronounced when enforced by the application of current pulses at low temperatures. Metastable states are characterized by long-term memory surviving even thermal cycling to room temperatures. Only heating to $T>T_e\approx 350$ K erases the previously imprinted state of the system. At temperatures close to the low temperature resistivity maximum, a slow relaxation of the resistance has been observed following changes in the bias current. Ac susceptibility, low-field magnetization, and specific heat data indicate that there is a spin-cluster glass-like transition at temperatures corresponding to the maximum of the relaxation time. Phase separation and coexistence of metallic and insulating ferromagnetic phases with different orbital order at a wide temperature range are claimed to be responsible for the observed electric-field and current effects. The disappearance of the resistance memory effects at temperatures above $T_e$ may be considered an indirect proof for the existence of one more temperature scale in disordered manganites.

DOI: 10.1103/PhysRevB.70.064414 PACS number(s): 75.47.Gk, 71.30.+h, 75.47.Lx, 76.90.+d

## I. INTRODUCTION

Manganite perovskites $La_{1-x}Ca_xMnO_3$ (LCMO) are characterized by a complex phase diagram containing a rich variety of magnetic and electronic phases. The ground state of low Ca-doped, $x<0.07$, LCMO is canted antiferromagnetic (AFM) insulator. For a doping level contained within the $0.07<x<0.22$ range, a dominant ferromagnetic insulating (FMI) ground state appears. For $0.22<x<0.5$ the ground state becomes a ferromagnetic metallic (FM) state.[1] Double exchange (DE) interaction is claimed to be responsible for establishing ferromagnetism in LCMO through a strong Hund's coupling between hopping $e_g$ electrons at neighboring $Mn^{3+}$ and $Mn^{4+}$ sites. However, for low doping levels, below the percolation threshold,[3] $x<x_C\approx 0.22$, an additional FMI phase, incompatible with the DE mechanism has been observed.[3–6]

According to recent theoretical[7,8] and experimental[4–6,9] studies, the superexchange (SE) interactions and orbital ordering (OO) may govern the transport and magnetic properties of low-doped manganites along with the DE interactions. Neutron diffraction,[10] NMR,[4,5,11] magnetization,[12,13] and Mössbauer[14] data indicated that LCMO samples with $0.125\leqslant x\leqslant 0.2$ undergo an additional phase transition at $T\approx 70-80$ K well below the para-to-ferromagnetic transition at Curie temperature $T_C$. The additional phase transition is accompanied by a number of peculiar features, such as strong frequency dependence of the ac susceptibility,[12,13] remarkable rotation of the easy magnetization axis,[13] wipeout of the $^{139}La$ NMR signal upon heating,[4,11] and reduction of the orthorhombicity at temperatures below the critical point.[10] An ensemble of these features is considered to be a fingerprint of the cluster spin-glass transition specific for disordered manganites.[2,15]

However, the most prominent feature, which is likely responsible for most of the peculiar properties of perovskite manganites, including the colossal magnetoresistance (CMR) effect, is the pronounced phase separation (PS) in a wide temperature range, leading to a dynamic coexistence of various phases with different properties.[1,2] Competition between magnetic and orbital ordering of coexisting phases may result in the appearance of metastable states manifesting themselves in metastable conductance,[16,17] nonequilibrium and nonstationary magnetization slowly relaxing after changes in the applied magnetic field,[16,18] or two-level noise and resistance memory effects.[17,19,20] The overwhelming majority of experimental evidence of the relaxation processes and metastable states is based on the effects related to changes in the applied magnetic field.[18,21–23] We have previously reported on the appearance of a rich variety of metastable states induced by means of electric-field and current procedures in $La_{0.8}Ca_{0.2}MnO_3$ single-crystalline samples.[17] Specific electric bias procedures generally caused a reduction of the pristine resistivity and resulted in the appearance of reproducible structures in the $I$-$V$ curves.

In this paper we report on experimental investigations of current-induced and spontaneously created metastable and nonequilibrium states in $La_{0.8}Ca_{0.2}MnO_3$ single crystals in

 

which the metastable resistance significantly exceeds the pristine state one. In particular, we concentrate on slow resistivity relaxation at low temperatures and resistance memory effects. To get a deeper insight into physics associated with metastable resistivity we have also performed additional magnetic and calorimetric measurements.

## II. EXPERIMENTAL DETAILS

The experiments were performed with $La_{0.8}Ca_{0.2}MnO_3$ single crystals grown by a floating zone method, as described elsewhere.[24] As-grown crystals were cut into individual samples for resistive and magnetization measurements. Samples for the resistivity measurements were prepared in the form of $8\times3\times1.6$ mm$^3$ bars, having the longest dimension along the ⟨110⟩ crystallographic direction. Current and voltage leads were indium soldered to the pre-evaporated gold contacts.

Measurements of current-voltage characteristics ($I$-$V$) and differential resistance ($R_d=dV/dI$) were made at zero applied magnetic field in a standard four-point arrangement. The separation between the voltage contacts was of the order of 1 mm. We have used 10 $\mu$A at 613 Hz current modulation for the phase sensitive lock-in $R_d$ measurements. $R(T)$ characteristics were measured in a dc mode using 20–100 $\mu$A current flow. The resistance measurements in applied magnetic field were performed for the field directed parallel to the current direction.

In addition to the transport measurements, series of magnetic and calorimetric measurements have been performed. Magnetization measurements have been performed in the temperature range 4.2–220 K by means of a vibrating sample magnetometer. The specific heat was measured by means of the relaxation method, using a specific heat option of the Quantum Design physical property measuring system (PPMS).

## III. RESULTS AND ANALYSIS

Low temperature resistivity of $La_{0.8}Ca_{0.2}MnO_3$ single crystals, like that of other lightly Ca-doped $La_{1-x}Ca_xMnO_3$ compounds, strongly depends on magnetic, thermal, and current bias history of the sample. Moreover, similar to a previously reported case of $La_{0.82}Ca_{0.18}MnO_3$,[17] the $La_{0.8}Ca_{0.2}MnO_3$ samples undergo spontaneous or external stimuli enforced transitions to metastable states characterized by markedly different resistivity. Figure 1 illustrates the temperature evolution of the resistance of $La_{0.8}Ca_{0.2}MnO_3$ crystal recorded at zero applied magnetic field and at $H=14.5$ kOe. The lower resistivity curves were recorded during cooling down the sample in the pristine state, while the high resistivity curve follows the evolution of one of metastable states. Zero field recordings exhibit a pronounced maximum at temperature coinciding within the experimental error, with the Curie temperature evaluated from independent magnetization data $T_C=184$ K.[13] All $R(T)$ curves exhibit a minimum at $T\approx140$ K, followed by a subsequent resistivity upturn at low temperatures. The upturn ends in a broad maximum located at $T\approx70$ K, after which the resistivity slowly drops to the low temperature finite value.

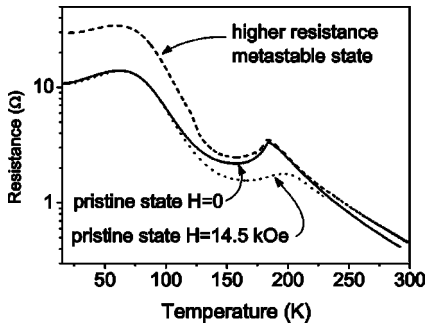


FIG. 1. Temperature dependence of the resistance of $La_{0.8}Ca_{0.2}MnO_3$ crystal measured with 100 $\mu$A dc current. Solid line: pristine resistive state at $H=0$, dotted line: pristine state at 14.5 kOe applied parallel to the current flow direction along ⟨the ⟨110⟩ crystallographic axis, dashed line: higher-resistivity metastable state created by current procedures at low temperatures, see text.

The LCMO sample may spontaneously jump to a higher resistivity metastable state when maintained for a long time at low temperatures close to the low temperature resistivity maximum. The probability of such a transition is strongly enhanced by extensive bias current and/or magnetic field sweeping, as well as by repeated thermal cycling between low and room temperatures.

A freshly established metastable state exhibits strong instabilities and resistivity jumps as shown in Fig. 2. Sometimes it may even spontaneously return to a pristine state. An example of such a reentrant transition recorded during sweeping of the magnetic field is presented in the inset to Fig. 2. With continuing thermal or bias cycling, the resistivity jumps and reentrant transitions became more rare and eventually disappear after a few cycles, leaving the sample in the long-lifetime higher-resistivity metastable state.

Metastable resistivity in $La_{0.8}Ca_{0.2}MnO_3$ samples can be spontaneously established during thermal or bias cycling.

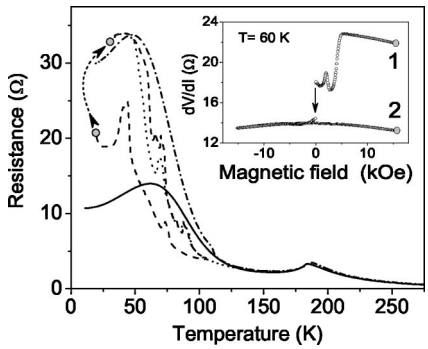


FIG. 2. Pristine state resistance (solid line) and evolution in time of the freshly established higher resistivity metastable state during subsequent thermal cycles marked with dashed, dotted, and dashed-dotted lines. Note the extended instabilities and resistance jumps. The inset shows an example of a spontaneous transition from a freshly established higher-resistive state to a pristine state. The points labeled 1 and 2 mark the start and the end of the magnetic-field cycle. The arrow indicates a jump in the dynamic resistance.

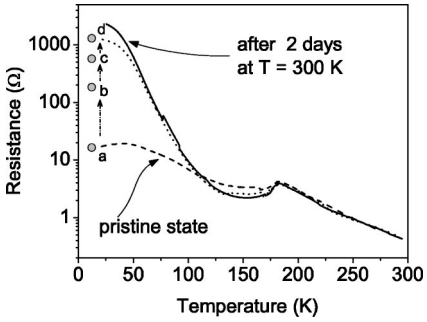


FIG. 3. Pulse enforced transition to high resistivity state at $T=10$ K. Dashed line: cooling down of the sample in the pristine state. Application of 10 V, 10 ms voltage pulse to the sample at the point (a) rises the resistance to the level labeled as (b). The subsequent two pulses increase further the resistance to the levels marked (c) and (d). The maximum current in each voltage pulse has been limited to 40 mA. The pulse-treated sample has been brought from low to the room temperature along the dotted curve. The pulse-induced metastable state has a strong memory of its state as indicated by the solid curve recorded after storing the previously pulse-treated sample at room temperatures for more than 48 h.

However, it turned out that an even more pronounced high resistivity metastable state can be enforced by biasing the sample with a series of voltage/current pulses at low temperatures. An example in which a metastable state has been induced by a pulse treatment is illustrated in Fig. 3. Here, we have applied three subsequent voltage pulses with 10 V amplitude and 10 ms length to the sample cooled down to 10 K in the pristine state. The maximum current within each pulse was power supply limited to a maximum of 40 mA. As seen in Fig. 3, this treatment causes a progressive increase of the resistance from the initial pristine 10 Ω range to 2.5 kΩ, i.e., by three orders of magnitude.

The metastable states are characterized by a relatively long lifetime, significantly exceeding the time scale of an experiment. In practice, only heating of the sample above $T=T_e\approx 350$ K can erase the memory and rejuvenate the resistance to the pristine state. The strength of the memory effect is illustrated by a solid line in Fig. 3, showing the temperature evolution of the resistance of a sample that has been pulse treated at low temperature, brought to the room temperature, and maintained for more than two days at 300 K.

Magnetoresistance (MR) of $La_{0.8}Ca_{0.2}MnO_3$ strongly depends on temperature, see Fig. 4. At temperatures well above $T_C$, when the sample is in the paramagnetic state, MR is practically absent. The most pronounced MR is observed, as expected, in the vicinity of the metal-insulator (MI) transition, see Fig. 1. At low temperatures below $T_C$ the MR is negligible to reappear again only as weak reentrant negative MR effect around the resistivity maximum at $35\ \mathrm{K}<T<120$ K. In this temperature range we also observe a significant magnetic hysteresis that is absent at other temperatures, as illustrated in Fig. 4. Eventually, at low temperatures, below 35 K, the magnetization and resistance are almost constant and MR does not exceed 1% for magnetic fields up to 15 kOe, the maximum field available in this experimental setup.

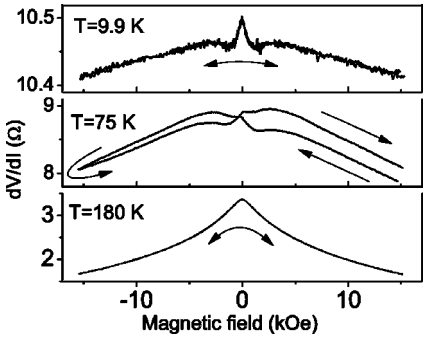


FIG. 4. Dynamic resistance of the pristine state vs magnetic field at various temperatures.

The open MR hysteresis loop recorded at 75 K (Fig. 4) indicates that the observed hysteresis is not due to a real magnetic hysteresis, but is rather caused by nonstationary resistivity, which relaxes following changes in the applied magnetic field. In fact, in the same temperature range we have observed hysteretic behavior of the resistivity, as illustrated in Fig. 5, showing the dynamic resistance of a pristine state sample during several consecutive slow current cycles between the maximum positive and negative values. After bringing the current back to zero the resistance slowly relaxes to an equilibrium value of the starting point, as indicated by a double arrow in Fig. 5.

Resistivity relaxation has been seen directly after an abrupt turning on and off of dc current of relatively low density, as illustrated in the inset to Fig. 6. The relaxation rate of the resistivity depends on the height of the current step, temperature, and the state at which the relaxation is observed. In general, the relaxation rates in more resistive states are slower. It is apparent that the relaxation rates observed in a given state after turning on and off the same current are identical.

Low-temperature nonstationary processes, in the form of slow relaxation of the magnetization and resistivity after steplike changes of the magnetic field, were widely reported in the literature.[18,25–28] To describe the resistance relaxation we have used the same stretched exponential formula that was commonly employed to describe the magnetization and resistivity relaxation processes in manganites after steplike changes of the applied magnetic field

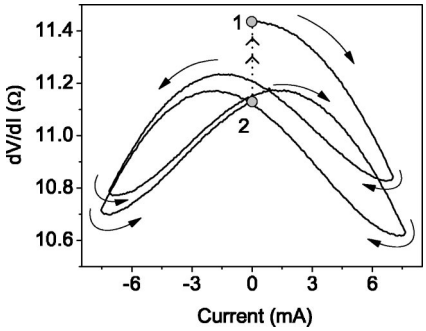


FIG. 5. Evolution of the pristine state dynamic resistance during cycling of the bias current at 80 K. Current sweep starts at point 1. After stopping the sweep at point 2 the resistance slowly relaxes back to initial point 1, as marked by a double arrow.

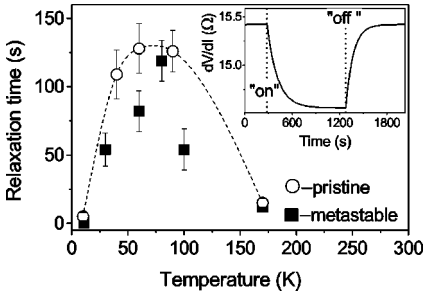


FIG. 6. Temperature dependence of the characteristic relaxation time $\tau$ for a pristine, and one of the higher resistivity metastable states. The line is a guide to the eye. Inset: exponential relaxation of the dynamic resistance after turning on and off 10 mA dc current step at 40 K. The instants of turning on and off the current are marked with dotted lines.

$$R(t) = R_0[1 \pm \exp(-\tau/t)^{\beta(T)}], \tag{1}$$

where $\tau(T)$ is a characteristic temperature-dependent relaxation time and $0<\beta<1$ is a dispersion parameter accounting for a distribution of the involved energy barriers, which causes the distribution of relaxation times in the system. Typically, $\tau(T)$ decreases exponentially and $\beta(T)$ increases linearly with increasing temperatures.[18,25–28] In our case, however, we have found that $\beta \approx 1$ and the current-induced relaxation process can be well described by a single relaxation rate. The experimentally determined temperature dependence of $\tau(T)$, as observed in the pristine and one of the higher resistivity metastable states, is shown in Fig. 6. Note that the relaxation time reaches the maximum between 75 and 85 K.

Surprisingly, no relaxation of resistance has been observed when the sample was directly immersed into the liquid-nitrogen bath. This fact suggests that heat dissipated by current flow may be responsible for the observed resistance relaxation. If this is indeed the case, then one would expect that either the heat capacity of our sample follows the temperature evolution of the relaxation rate and exhibits a maximum at temperatures for which the time required to reach the thermal equilibrium in our samples reaches the maximum, or the heat conductivity of the sample should exhibit a minimum in the temperature range coinciding with the maximum of the relaxation time. To enlighten this problem we have performed calorimetric measurements in the temperature range 2–300 K in zero applied magnetic field and in $H=70$ kOe. The results presented in Fig. 7 show a singularity at the temperature of the paramagnetic-to-ferromagnetic phase transition. The peak position corresponds to the Curie temperature $T_C$ and MI transition at the resistivity peak in Fig. 1. However, our data do not show any anomaly in the temperature range, where the maximum in the relaxation time has been observed. Although we could not measure directly the heat conductivity of our sample, nevertheless, any anomaly in the heat conductivity should be also reflected in the relaxation time of the thermal exchange between the sample and calorimeter. This quantity has been carefully measured and did not show any anomaly in the investigated temperature range.

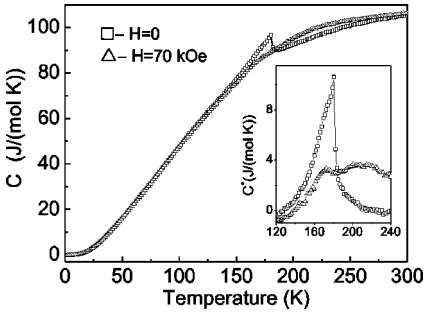


FIG. 7. Heat capacity of the $La_{0.8}Ca_{0.2}MnO_3$ crystal as a function of temperature in zero magnetic field (squares) and in $H=70$ kOe (triangles). The inset shows the excess part of the specific heat, obtained by subtracting the smooth background contribution from the specific heat in the vicinity of the paramagnetic-to-ferromagnetic phase transition. Note the pronounced λ shape of the zero-field curve.

Specific heat data obtained during cooling and heating runs practically coincide, both for $H=0$ and 70 kOe. The lack of thermal hysteresis around $T_C$ may be seen as signature of the second-order type of FM to paramagnetic (PM) phase transition. To get a better insight into the character of this phase transition we have subtracted the smooth background, obtained by polynomial fitting, from the data around the peak. The remaining excess part of the heat capacity, $C^*$, has a well-pronounced λ-shaped form, see inset to Fig. 7, confirming that the discussed phase transition is of the second order.

The proportionality of the specific heat to the temperature coefficient of the resistivity $dR/dT$ in the vicinity of $T_C$, see Fig. 8, proves the magnetic character of the specific heat peak as expected for a Fisher-Langer–type anomaly associated with a decrease in spin disorder scattering below the transition temperature.[29] Applied magnetic field orders spins in the transition zone, resulting in the disappearance of the specific heat peak and smoothing of the $R(T)$ characteristics. With decreasing temperature the $dR/dT$ characteristics show a rich structure, which is not repeated in the specific heat, indicating that the Fisher-Langer scenario cannot be applied in the temperature range of the resistivity relaxation.

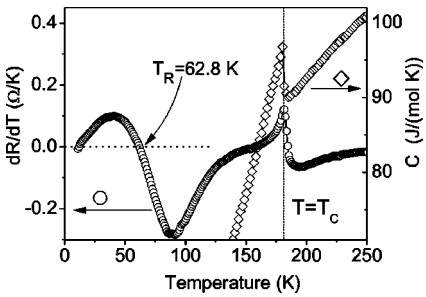


FIG. 8. Specific heat measured at zero magnetic field is proportional to $dR/dT$ in the vicinity of the para-to-ferromagnetic phase transition. Characteristic temperature $T_R$ at which $dR/dT=0$ marks the inflexion point of the low temperature reentrant part of the $R(T)$ characteristics. The dotted line is placed at $T=T_C$ determined from the magnetization measurements.

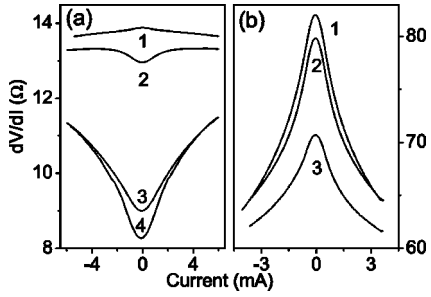


FIG. 9. (a) Dynamic resistance vs current of a pristine state sample subjected to different cooling procedures and pulsed current treatments. Curve 1—after quick cooling (direct immersion in liquid $N_2$); curve 2—after relatively slow cooling to 100 K with the rate of about 3 K/min and subsequent immersion into liquid $N_2$ bath; curve 3—after a quick cooling and subsequent application of a train of current pulses (+40 to −40 mA); curve 4—obtained from curve 3 after application of an additional current pulse (+40 to −40 mA) at $H=5$ kOe. (b) Dynamic resistance vs current for high-resistivity metastable state obtained by means of pulse current treatment at 10 K. Curve 1—after slow (rate$\approx$3 K/min) cooling to 100 K followed by a direct immersion in liquid $N_2$; curve 2 — obtained from curve 1 after application of a current pulse (+40 to −40 mA); curve 3— obtained from curve 2 after application of one more current pulse.

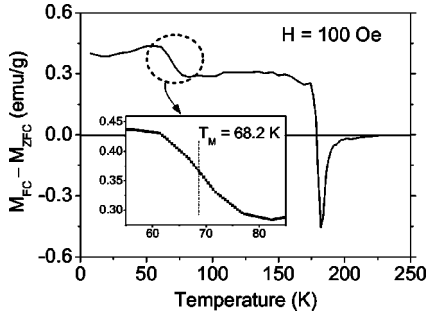


FIG. 10. The difference between FC and ZFC low-field magnetization as a function of temperature. A broad step at low temperatures is enlarged in the inset. The inflexion point of the experimental $\Delta M(T)=M_{FC}-M_{ZFC}$ curve is at 68.2 K.

The final blow to the heating scenario came from the observation that resistance was decreasing after a steplike increase of the dc current, not only in the temperature range of the resistivity upturn, where $d\rho(T)/dT<0$ and a small increase of the sample temperature due to the heat dissipated by current flow could explain slow resistivity decrease, but also at temperatures below the low temperature resistivity peak, where $d\rho(T)/dT>0$. We have observed a reduction of the resistance after turning on the current also at the temperatures below the low temperature resistivity peak. A simple heating mechanism should result in an increase of the sample resistance with increasing temperature, contrary to the experimental reality. Consequently, the lack of resistivity relaxation in samples immersed directly into liquid-nitrogen bath cannot be explained by a high efficiency of cooling through a direct contact with a liquid cryogen. This effect should be rather attributed to the very high cooling rate in the final stage of cooling at which samples reach the liquid-nitrogen temperature.

It has been already demonstrated that the sample resistivity strongly depends on the cooling rate with which the phase transition has been crossed.[16,18,21,22] The underlying physical reason is the degree of phase separation that depends on the cooling rate. We have found that in $La_{0.8}Ca_{0.2}MnO_3$ crystals it is not only the resistivity, but also the shape of the current-voltage characteristics $I$-$V$, that strongly depends on the cooling rate and specific bias procedures. Figure 9(a) shows $R_d(I)$ characteristics recorded after dropping a pristine state sample directly into the liquid nitrogen, curve 1. The characteristics of the same sample immersed into the cryogen bath after relatively slow precooling with the rate of 3 K/min is shown in curve 2. The difference between both $R_d(I)$ characteristics is particularly pronounced in the vicinity of zero bias. In the quenched sample the resistivity decreases with increasing current, while the opposite behavior is seen in the slowly cooled sample. Application of two subsequent 40 mA amplitude, 10 ms current pulses with different polarities reduces the resistivity of the quenched pristine state and converts it to a lower resistivity metastable state, see curve 3, similar to what has been previously observed in $La_{0.82}Ca_{0.18}MnO_3$.[17] Additional current pulses applied in the presence of 5 kOe magnetic field further reduces the resistivity, see curve 4. In a marked difference, the dynamic resistivity of high resistivity metastable state (2.5 kΩ at $T=10$ K) created by means of pulse treatment at $T=10$ K strongly decreases with increasing current. Moreover, application of analogous current pulse procedures to the sample in very high resistivity metastable state leads to subsequent decreases of the resistance, see Fig. 9(b).

It is worth underlining that metastable states in our experiments could be created and modified only at low temperatures below the onset of the resistivity relaxation. The onset temperature coincides roughly with the temperature of the broad resistivity minimum. The following low temperature resistivity reentrance is accompanied by peculiar features reminiscent of glassy freezing, such as a remarkable difference between field-cooled (FC) and zero-field-cooled (ZFC) dc magnetization at low fields, and a steep decrease and frequency dependence of the ac susceptibility.[30–32]

Magnetization measurements show that in $La_{0.8}Ca_{0.2}MnO_3$ samples ZFC magnetization starts to deviate from the FC value immediately below $T_C$.[13] However, within a narrow temperature range, which roughly coincides with the appearance of the maximum in relaxation times, there is an additional slow increase of FC magnetization with decreasing temperature accompanied by a slow decrease of ZFC magnetization. The resulting broad smeared steplike feature is shown in Fig. 10, in which the difference between ZFC and FC magnetization measured at 100 Oe is plotted as a function of temperature. The first sharp and narrow feature on the $\Delta M(T)$ curve in Fig. 10 coincides with the MI transition at $T_C$. A significant difference between ZFC and FC magnetization just below the magnetic ordering transition may be related to changes in the magnetic anisotropy and coercive field.[33] An additional broad increase of the magnetization difference at low temperature is centered at $T=68.2$ K, as determined as the inflexion point of the $\Delta M(T)$ curve.

As shown in our previous report,[13] the real and imaginary part of ac magnetic susceptibility became frequency dependent at temperatures below $T_C$. The $\chi'$ curves show pronounced cusps that move to higher temperatures with increasing frequency. The cusps in $\chi''(T)$ are accompanied by a sharp drop in $\chi'(T)$ characteristics occurring at the same temperature. The onset of decrease of the real part of ac susceptibility also moves to higher temperatures with increasing frequency. This frequency-dependent temperature shift can be attributed to relaxation phenomena in the spin system and characterized by a factor

$$K = \frac{\Delta T_{cusp}}{T_{cusp}\Delta(\lg\omega)}, \tag{2}$$

where $T_{cusp}$ refers to the temperature of the maximum in $\chi(T)$ curve and $\Delta T_{cusp}$ to the cusp position difference observed at a given frequency difference. The calculated value of the $K$ factor for our $La_{0.8}Ca_{0.2}MnO_3$ sample is 0.035, which falls in the range typical for spin glasses.[15]

In conventional spin glasses the critical slowing down is characterized by a relaxation time $\tau$, which diverges at the critical freezing point as[15]

$$\tau_{max} = \tau_0\left(\frac{T_f - T_G}{T_G}\right)^{-z\nu}, \tag{3}$$

where $\tau_0$ is the shortest relaxation time available in the system, $z$ is the dynamic exponent, $\nu$ is spin-correlation length exponent, $T_G$ is the glass transition temperature, and $T_f$ is the freezing temperature. The typical values of $\tau_0$ are of the order of the time of a flip of a single spin atomic magnetic moment and lie between $10^{-12}$–$10^{-14}$ s. By identifying $\tau_{max}$ with the inverse of the measuring frequency and the cusp temperature of the frequency dependent susceptibility curves with freezing temperature $T_f$, we have obtained from the nonlinear fit to Eq. (3) $\tau_0 = 10^{-12}$ s, $z\nu = 12$, and the transition temperature $T_G = 66.7$ K. It is interesting to note that similar fitting procedures performed with the susceptibility data obtained with $La_{0.82}Ca_{0.18}MnO_3$ single crystals,[12] rendered the same values of $\tau_0$ and $z\nu$ parameters. The only difference between these two systems was a higher $T_G = 71.8$ K parameter for $La_{0.82}Ca_{0.18}MnO_3$.

Although the presumed spin-glass-like transition does not manifest itself as a singularity on the temperature dependence of the heat capacity, the difference between specific heat measured in zero magnetic field and in the field of 70 kOe, plotted in Fig. 11, supplies a more direct indication of the presence of a transition in the vicinity of the spin-glass freezing temperature. The large, high-temperature anomaly in $\Delta C = C(H) - C(H=0)$ is associated with the ferromagnetic transition at $T = T_C$. At lower temperatures $\Delta C$ seems to decrease to zero monotonically, as expected for systems with just one paramagnetic-ferromagnetic phase transition.[34] However, a more detailed analysis of the spin glass freezing temperature range reveals the presence of an anomaly and a significant difference in the behavior of $\Delta C$ at temperatures below and above $T_G$. The inset shows $\Delta C$ from which the background contribution, obtained by a polynomial fit to the low temperature part of the dependence, has been subtracted

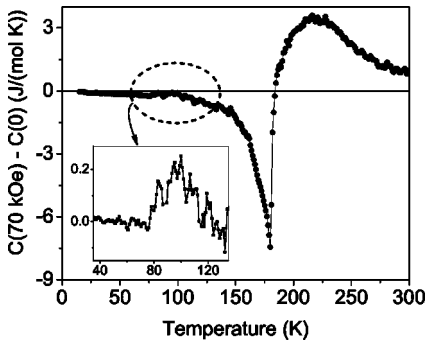


FIG. 11. The difference between specific heat measured at $H = 70$ kOe and at zero magnetic field as a function of temperature. The inset shows an enlarged part of the main graph, enclosed by the dashed ellipsoid, from which the background contribution has been subtracted.

in an expanded scale. The revealed excess $\Delta C$ at the spin-glass transition is 0.23 J/mol$K$, which is indeed very small as compared to the analogous specific heat difference peak $\Delta C = 7$ J/molK at the para-to-ferromagnetic transition, see Fig. 7. Most likely it is unfreezing of the spin-glass state that provides an additional small contribution to the zero field specific heat at this transition point.

We want to stress that it is very difficult to separate magnetic contribution to specific heat in spin-glass systems from overwhelming phonon and electron contributions at temperatures exceeding the level of a few kelvin.[15] Only the specific differential procedure presented above enabled us to reveal the presence of the spin-glass transition in the specific heat data at higher temperatures.

## IV. DISCUSSION

The ensemble of experimental results univocally indicates that the system undergoes glassy freezing at temperatures close to experimentally determined $T_G$. Manganites are known not to behave like canonical spin glasses.[15] The glassy behavior in manganites is strongly related to phase separation and dynamic coexistence of magnetically distinct phases.[2,25] Phase separation and associated randomness in position of the spins, together with competing or mixed interactions, causes frustration, thus providing the most important prerequisite for the spin-glass-like behavior. Since the dominant interactions leading to frustration occur between nanoscopic phase-separated clusters, the glassy state in manganites is referred to as a cluster spin glass, see Ref. 2 and references therein.

Resistance metastability, memory, relaxation, and spin-glass-like freezing are apparently interconnected. One can create and modify metastable states only at temperatures below the onset of observable resistance relaxation and appearance of the spin-glass freezing hallmarks. Moreover, spin-glass transition temperature $T_G = 66.7$ K, determined from the susceptibility data, coincides with the maximum of the relaxation time. $T_G$ is very close to the characteristic magnetization temperature $T_M = 68.2$ K, marking the center of a broad steplike increase of the magnetization difference be-

tween ZFC and FC processes, see Fig. 10, and to the characteristic resistance temperature $T_R = 62.8$ of the center of low-temperature resistivity reentrance determined in Fig. 8. The temperature range of the pronounced resistivity relaxation contains, as well, the temperatures at which the temperature dependence of the difference between specific heat measured in the presence of magnetic field and in zero field changes character and $\Delta C$ goes through a local maximum.

The transition at $T_G$ can be interpreted in two complementary ways. Papavassiliou *et al.*[5] concluded from the analysis of $^{55}$Mn and $^{139}$La NMR data that freezing into inhomogeneous OO state constituted by FM insulating domains, separated by FM metallic walls, occurs at $T = T_{tr}$, which is very close to our $T_G$. From a structural point of view, the orbitally ordered ($O'$) and orbitally disordered ($O*$) phases coexist in a wide temperature range, starting from the ordering temperature $T_{O'-O*}$ up to the temperatures much higher than the Curie temperature $T_C$. This coexistence may be characterized by the Q2 orthorhombic distortion, with in-plane bonds differentiating in long and short one, namely the changes in structure due to OO are described using the Q2 distortion.[9] Careful x-ray diffraction analysis has shown that the Q2 distortion is constant below $T_{O'-O*}$ and decreases smoothly above $T_{O'-O*}$ both in paramagnetic and ferromagnetic phases. Comparing Ca-doping dependence of $T_{O'-O*}$[9] with that of dependence of $T_{tr}$[4,5] one may conclude that the temperatures $T_{O'-O*}$, $T_{tr}$, and $T_G$ relate to the very same transition seen through different experimental results.

The low-doped LCMO system is unique among other manganite systems because its phase-separated ground state contains two phases with the same magnetic, but different orbital order. Effective Hamiltonian including orbital, spin, and charge degrees of freedom provides a phase-separated state constituted by two ferromagnetic phases.[8] In the first phase an antiferrodistorsive-type OO is favored by FM superexchange interactions through coupling between spin and orbital degrees of freedom of $e_g$ electrons.[8] For the second FM phase the ferrodistorsive-type OO promotes double exchange interactions by gaining in the kinetic energy. Recent NMR[4,5] and structural[9] investigations of low-doped LCMO samples have confirmed the above model. Therefore, it is now a well-established fact that two FM phases with distinct OO and different conductivity coexist in a wide temperature range.[2,4,5,9,10,35]

There are several reports[18,21–23,25–28] on relaxation phenomena in manganites observed after changes in the applied magnetic field. These procedures affect directly the magnetic order of the sample. Both magnetization and resistance relaxation have been observed. Our experimental results demonstrate resistivity relaxation, metastability, and long-term resistance memory due to electric-field (bias current) procedures, and are complementary to previously reported effects of abrupt and slow changes of applied magnetic field. The similarity between the effects of low-density currents and relatively strong magnetic fields upon the resistivity of lightly Ca-doped manganites have already been described by us for the stationary case.[36] Current experiments extend the equivalence between the effects of strong magnetic fields and weak electric currents and fields to nonstationary processes as well.

Phase separation and coexistence of two phases with different conductivity is a key element for understanding the experimental results. The resistivity of the PS system does not depend solely on the ratio of the volumes of coexisting phases, but also in a crucial way depends on the distribution of the conductive domains and their size and shape.[37] At the various stages of the percolation of conductive domains the system could be "more insulating" or "more metallic," as is illustrated by a difference in behavior of pristine, low-resistivity, and highly-resistive metastable states upon application of current scans.

The dependence of the resistive state on cooling conditions follows in a natural way from the properties of the PS state. Previously reported FM Bragg peak intensity[10] of $La_{0.8}Ca_{0.2}MnO_3$ crystal at low temperatures has been attributed to the nucleation or rearrangement of orbital domains, which depends on the cooling rate.[9] When FM metallic and charge ordered insulating phases coexist, as in the case of $La_{0.5}Ca_{0.5}MnO_3$, slow cooling through $T_C$ favors the conductive phase and results in a lower resistance of the sample.[16] In our case, slow cooling of $La_{0.8}Ca_{0.2}MnO_3$ through $T_C$ also favors a more conductive phase. The lack of observable resistivity relaxation and different form of $I$-$V$ curves in samples directly immersed into liquid nitrogen can be also related to the cooling rate. Although there was no significant difference between slowly cooled and rapidly cooled samples it should be underlined that the major influence of the cooling rate is related to the speed of crossing the phase-transition temperature. The "slow cooled" samples were slowly cooled to 100 K and then abruptly brought into contact with the liquid cryogen at 77 K. Therefore, even if the magnetic ordering phase transition has been crossed slowly, the samples were rapidly quenched through the first stage of the freezing spin-glass transition. Unfortunately, technical difficulties prevented us from performing an experiment in which samples would be cooled slowly, with the same speed, down to the immersion in a liquid-nitrogen bath.

Electric field may directly affect the directional order of orbitals and thus alter the magnetic state, when the compound is insulating enough.[7] Another way in which electric current may influence the magnetic order and conductivity is by direct injection of spin-ordered electrons to specific phase separated domains by means of spin-polarized current. It has been shown that effects of weak and strong magnetic fields upon the PS state are related to two different relaxation mechanisms. Weak magnetic fields cause reorientation of ferromagnetic domains, while strong fields change the topology of the PS state.[25] By analogy, we propose to distinguish the effects of weak and strong currents. The dominant effect of weak currents likely consist in reversible injection of the spin-polarized carriers into specific ferromagnetic domains, thus increasing the volume of one phase on the expense of the other, while the strong current will act by means of the associated strong electric field capable of inducing local changes to the orbital order in the less conducting phase and/or electric field enforced changes of the topology of the phase coexistence. Namely, for this reason, the effects of the electric field and current became pronounced only at low temperatures, where the conductivity of distinct ferromagnetic phases becomes sufficiently different to allow for a

selective interaction between electric field and PS clusters.

Experiments with various manganite systems have proved that electric field and current can destabilize or even completely destruct a charge or orbitally ordered state.[38,39] In general, the orbital ordering and metalliclike conductivity are mutually exclusive. Therefore, transport properties of the $La_{1-x}Ca_xMnO_3$ system are strongly influenced by nucleation and rearrangement of orbitally ordered domains, especially in the vicinity of the orbital order-disorder transition, when energies of ordered and disordered phases are comparable and spontaneous transitions between them are possible. Then, moderate electric current and field easily induces rearrangements of orbital domains and domain walls either by means of spin-polarized current flow or by direct interaction with elastic forces. This process is obviously not instantaneous and the relevant time delays will manifest themselves in the relaxation of the resistivity. The strong dependence of the resistivity on the cooling procedure (Fig. 9) is in agreement with the results of neuron measurements, which revealed metastabilty in both magnetic and structural characteristics for low-doped $La_{1-x}Ca_xMnO_3$.[10]

The orbital distortion is stabilized by strong magnetoelastic forces and can be eliminated from the system only by completely removing all nuclei of the influenced phase. In $La_{0.8}Ca_{0.2}MnO_3$ this occurs only when the sample is heated above the memory erasing temperature $T_e \sim 350$ K. This temperature coincides with the upper limit of the orbitally ordered-disordered phase coexistence as determined from the structural measurements[9] as well as with the upper limit of the existence of the vibronic conductivity proposed by Goodenough.[35] In the latter scenario two-manganese Zener polarons progressively condense on cooling as a result of a spinodal phase segregation into hole-rich ferromagnetic vibronic (FV) clusters within paramagnetic orbitally ordered or disordered matrix. The concentration of hole-rich clusters increases with increasing doping level $x$ and with decreasing temperature. Below a critical temperature $T_{sp} > T_C$ they become superparamagnetic ferromagnetic vibronic conductivity clusters.[35] Even, if $T_{sp}(x)$ has not been systematically mapped by experiment, for $La_{0.8}Ca_{0.2}MnO_3$ $T_{sp}$ coincides with the temperature of disappearance of the Q2 distortion, compare the phase diagrams published in Refs. 35 and 9. The existence of yet another temperature scale follows also in a natural way from a general model of a clustered states in disordered solids.[2] This upper temperature limit can be identified as the Griffiths temperature $T^*$, which in our case coincides with $T_e$.

## V. CONCLUSIONS

We have shown that even relatively weak electrical currents can induce strong changes in the resistivity of $La_{0.8}Ca_{0.2}MnO_3$ single crystals. Current pulses applied at low temperatures induce metastable resistivity states characterized by higher resistivity, with respect to the pristine state.

Phase separation has been found crucial to understanding the experimental data. Electric current/field influence the topology and the relative volume occupied by two coexisting ferromagnetic phases with different conductivity, due to differences in their orbital order.

The behavior of all distinct resistive states is strongly influenced by the cooling rate and previous magnetic and electric bias history of the sample. Pronounced exponential resistivity relaxation following changes in the applied current flow has been observed in the temperature range coinciding with the low-temperature resistivity upturn. Several concomitant phenomena enabled us to identify a cluster spin-glass transition at $T_G$, which was found to coincide with several magnetic and resistive characteristic temperatures. We associate the glassy transition to the low-temperature orbital order-disorder transition.

Signatures of two phase transitions have been found in $La_{0.8}Ca_{0.2}MnO_3$ specific-heat data. The magnetic ordering transition turned out to be of the second order, where the excess specific heat follows the Fisher-Langer scenario. The magnetic contribution to the specific heat at the glassy transition has been evidenced in the difference between ZFC and FC behavior.

Current-induced metastable resistivity states are characterized by a long-term memory, surviving heating above Curie temperature $T_C$ and long-term storage at room temperatures. The system memory can be erased only by heating the sample above the temperature $T_e$, which was found to coincide with the experimentally determined upper temperature limit of the existence of Q2 distortion and theoretical critical temperature $T_{sp}$ of the transition to the vibronic ferromagnetic state. We believe that all these temperatures are manifestations of a temperature scale in doped manganites, which can be identified as a Griffiths temperature in a general scenario of clustered states in solid-state systems.

## ACKNOWLEDGMENTS

The assistance offered by M. Tsindlekht, I. Fita, and R. Puzniak in magnetic measurements is greatly acknowledged. This research was supported by the Israeli Science Foundation, administered by the Israel Academy of Sciences and Humanities (Grant No. 209/01), and by the European Commission under Project No. ICA1-CT-2000-70018 (Centre of Excellence CELDIS).

[1] E. Dagotto, T. Hotta, and A. Moreo, Phys. Rep. **344**, 1 (2001).

[2] E. Dagotto, *Nanoscale Phase Separation and Collosal Magnetoresistance*, Springer series in Solid State Physics (Springer, Berlin, 2003).

[3] T. Okuda, Y. Tomioka, A. Asamitsu, and Y. Tokura, Phys. Rev. B **61**, 8009 (2000).

[4] G. Papavassiliou, M. Belesi, M. Fardis, and C. Dimitropoulos, Phys. Rev. Lett. **87**, 177204 (2001).

[5] G. Papavassiliou, M. Pissas, M. Belesi, M. Fardis, J. Dolinsek, C. Dimitropoulos, and J. P. Ansermet, Phys. Rev. Lett. **91**, 147205

(2003).
[6] M. Hennion, F. Moussa, F. Wang, J. Rodriguez-Carvajal, Y. M. Mukovskii, and D. Shulyatev, cond-mat/0112159 (unpublished).
[7] Y. Tokura and N. Nagaosa, Science **288**, 462 (2000).
[8] S. Okamoto, S. Ishihara, and S. Maekawa, Phys. Rev. B **61**, 451 (2000).
[9] B. B. Van Aken, O. D. Jurchescu, A. Meetsma, Y. Tomioka, Y. Tokura, and T. T. M. Palstra, Phys. Rev. Lett. **90**, 066403 (2003).
[10] G. Biotteau, M. Hennion, F. Moussa, J. Rodriguez-Carvajal, L. Pinsard, A. Revcolevschi, Y. M. Mukovskii, and D. Shulyatev, Phys. Rev. B **64**, 104421 (2001).
[11] G. Allodi, M. C. Guidi, R. De Renzi, A. Caneiro, and L. Pinsard, Phys. Rev. Lett. **87**, 127206 (2001).
[12] V. Markovich, E. Rozenberg, A. I. Shames, G. Gorodetsky, I. Fita, K. Suzuki, R. Puzniak, D. A. Shulyatev, and Y. M. Mukovskii, Phys. Rev. B **65**, 144402 (2002).
[13] V. Markovich, I. Fita, R. Puzniak, M. I. Tsindlekht, A. Wisniewski, and G. Gorodetsky, Phys. Rev. B **66**, 094409 (2002).
[14] M. Pissas, G. Papavassiliou, E. Devlin, A. Simopoulos, and V. Likodimos, cond-mat/0403446 (unpublished).
[15] J. A. Mydosh, *Spin Glasses* (Taylor and Francis, London, 1993).
[16] M. Uehara and S.-W. Cheong, Europhys. Lett. **52**, 674 (2000); K. H. Kim, M. Uehara, V. Kiryukhin, and S.-W. Cheong, cond-mat/0212113 (unpublished).
[17] Y. Yuzhelevski, V. Markovich, V. Dikovsky, E. Rozenberg, G. Gorodetsky, G. Jung, D. A. Shulyatev, and Ya. M. Mukovskii, Phys. Rev. B **64**, 224428 (2001).
[18] P. Levy, F. Parisi, L. Granja, E. Indelicato, and G. Polla, Phys. Rev. Lett. **89**, 137001 (2002).
[19] Y. Yuzhelevski, V. Markovich, E. Rozenberg, G. Gorodetsky, G. Jung, D. A. Shulyatev, and Ya. M. Mukovskii, J. Appl. Phys. **91**, 7397 (2002).
[20] Y. Yuzhelevski, V. Dikovsky, V. Markovich, G. Gorodetsky, G. Jung, D. A. Shulyatev, and Ya. M. Mukovskii, Fluct. Noise Lett. **1**, L105 (2001).
[21] L. Granja, E. Indelicato, P. Levy, G. Polla, D. Vega, and F. Parisi, Physica B **320**, 94 (2002).
[22] R. Mathieu, P. Nordblad, A. R. Raju, and C. N. R. Rao, Phys. Rev. B **65**, 132416 (2002).
[23] A. Anane, J.-P. Renard, L. Reversat, C. Dupas, P. Veillet, M. Viret, L. Pinsard, and A. Revcolevschi, Phys. Rev. B **59**, 77 (1999).
[24] D. A. Shulyatev, A. A. Arsenov, S. G. Karabashev, and Ya. M. Mukovskii, J. Cryst. Growth **198/199**, 511 (1999).
[25] I. G. Deac, S. V. Diaz, B. G. Kim, S.-W. Cheong, and P. Schiffer, Phys. Rev. B **65**, 174426 (2002).
[26] J. Dho, W. S. Kim, and N. H. Hur, Phys. Rev. B **65**, 024404 (2001).
[27] I. Gordon, P. Wagner, V. V. Moshchalkov, Y. Bruynseraede, M. Apostu, R. Suryanarayanan, and A. Revcolevschi, Phys. Rev. B **64**, 092408 (2001).
[28] R. Ganguly, M. Hervieu, A. Maignan, C. Martin, and B. Raveau, J. Phys.: Condens. Matter **14**, 9039 (2002).
[29] M. E. Fisher and J. S. Langer, Phys. Rev. Lett. **20**, 665 (1968).
[30] K. Jonason, J. Mattsson, and P. Nordblad, Phys. Rev. B **53**, 6507 (1996).
[31] R. Laiho, E. Lähderanta, J. Salminen, K. G. Lisunov, and V. S. Zakhvalinskii, Phys. Rev. B **63**, 094405 (2001).
[32] R. Laiho, K. G. Lisunov, E. Lähderanta, P. Petrenko, J. Salminen, V. N. Stamov, and V. S. Zakhvalinskii, J. Phys.: Condens. Matter **12**, 5751 (2000).
[33] P. S. Anil Kumar, P. A. Joy, and S. K. Date, J. Phys.: Condens. Matter **10**, L487 (1998).
[34] S. Tsubouchi, T. Kyômen, and M. Itoh, Phys. Rev. B **67**, 094437 (2003).
[35] J. B. Goodenough, *Rare Earth-Manganese Perovskites*, Handbook on the Physics and Chemistry of Rare Earth, edited by K. A. Gschneidner, Jr., J.-C. G. Bünzli, and V. K. Pecharsky (Elsevier Science, Amsterdam, 2003), Vol. 33.
[36] V. Markovich, E. Rosenberg, Y. Yuzhelevski, G. Jung, G. Gorodetsky, D. A. Shulyatev, and Ya. M. Mukovskii, Appl. Phys. Lett. **78**, 3499 (2001).
[37] D. Khomskii and L. Khomskii, Phys. Rev. B **67**, 052406 (2003).
[38] J. Stankiewicz, J. Sese, J. Garcia, J. Blasco, and C. Rillo, Phys. Rev. B **61**, 11236 (2000).
[39] A. Asamitsu, Y. Tomioka, H. Kuwahara, and Y. Tokura, Nature (London) **388**, 50 (1997).